Advances in Radiation Oncology (2018) **3**, 331–338

advances
in radiation oncology

www.advancesradonc.org

Scientific Article

Radiomics-guided therapy for bladder cancer: Using an optimal biomarker approach to determine extent of bladder cancer invasion from t2-weighted magnetic resonance images

Yubing Tong PhD [a,1], Jayaram K. Udupa PhD, FIEEE, FAIMBE [a,1,*], Chuang Wang PhD [a], Jerry Chen MD [b], Sriram Venigalla MD [b], Thomas J. Guzzo MD [c], Ronac Mamtani MD [d], Brian C. Baumann MD [e], John P. Christodouleas MD [b,2], Drew A. Torigian MD, MA, FSAR [a,2]

[a] *Medical Image Processing Group, Department of Radiology, University of Pennsylvania, Philadelphia, Pennsylvania*
[b] *The Perelman Center for Advanced Medicine, Department of Radiation Oncology, University of Pennsylvania, Philadelphia, Pennsylvania*
[c] *The Perelman Center for Advanced Medicine, Department of Urology, University of Pennsylvania, Philadelphia, Pennsylvania*
[d] *The Perelman Center for Advanced Medicine, Department of Medicine, University of Pennsylvania, Philadelphia, Pennsylvania*
[e] *Washington University School of Medicine, St. Louis, Missouri*

Received 23 April 2018; accepted 28 April 2018

Abstract

Background: Current clinical staging methods are unable to accurately define the extent of invasion of localized bladder cancer, which affects the proper use of systemic therapy, surgery, and radiation. Our purpose was to test a novel radiomics approach to identify optimal imaging biomarkers from T2-weighted magnetic resonance imaging (MRI) scans that accurately classify localized bladder cancer into 2 tumor stage groups (≤T2 vs >T2) at both the patient level and within bladder subsectors.

Method and Materials: Preoperative T2-weighted MRI scans of 65 consecutive patients followed by radical cystectomy were identified. A 3-layer, shell-like volume of interest (VOI) was defined on each MRI slice: Inner (lumen), middle (bladder wall), and outer (perivesical tissue). An optimal biomarker method was used to identify features from 15,834 intensity and texture properties that maximized the classification of patients into ≤T2 versus >T2 groups. A leave-one-out

Conflicts of interest: There are no conflicts of interest.

Sources of support: This study was funded with grants from the Alan Wolson Fund at the Abramson Cancer Center, University of Pennsylvania in Philadelphia, Pennsylvania.

* Corresponding author: Medical Image Processing Group, Department of Radiology, University of Pennsylvania, 3710 Hamilton Walk, Goddard Building, 6th Floor, Rm 601W, Philadelphia, PA 19104.

E-mail address: jay@pennmedicine.upenn.edu (J.K. Udupa).

[1] Co-first authors.

[2] Co-senior authors.

https://doi.org/10.1016/j.adro.2018.04.011

strategy was used to cross-validate the performance of the identified biomarker feature set at the patient level. The performance of the feature set was then evaluated at the subsector level of the bladder by dividing the VOIs into 8 radial sectors.

Results: A total of 9 optimal biomarker features were derived and demonstrated a sensitivity, specificity, accuracy of prediction, and area under a receiver operating characteristic curve of 0.742, 0.824, 0.785, and 0.806, respectively, at the patient level and 0.681, 0.788, 0.763, and 0.813, respectively, at the radial sector level. All 9 selected features were extracted from the middle shell of the VOI and based on texture properties.

Conclusions: An approach to select a small, highly independent feature set that is derived from T2-weighted MRI scans that separate patients with bladder cancer into ≤T2 versus >T2 groups at both the patient level and within subsectors of the bladder has been developed and tested. With external validation, this radiomics approach could improve the clinical staging of bladder cancer and optimize therapeutic management.

Introduction

In the United States, an estimated 79,030 new cases of bladder cancer (60,490 men and 18,540 women) were diagnosed in 2017 and approximately 16,870 patients died of the disease.[1] For patients with localized bladder cancer, the major determinants of treatment are the presumed extent of invasion of the bladder primary tumor and its location within the bladder. If a primary tumor is known not to have invaded beyond the muscular wall (stage ≤T2), a patient may be treated adequately with bladder-directed therapies alone. However, if a primary tumor invades beyond the muscle wall (ie, extra-vesicle invasion or stage >T2), the patient requires more intensive systemic therapies and may benefit from pelvic lymph-node directed therapy.[2]

In addition, recent clinical protocols suggest that boost doses of radiation are directed only to subsectors of the bladder that likely harbor residual disease.[3] Unfortunately, the appropriate treatment of bladder cancer is limited by an inability to accurately determine both the extent of invasion and the location of tumors within the bladder preoperatively. With the present evaluation methods, a patient who is diagnosed with clinical T2 disease (ie, invasion into the muscle but not beyond) is almost equally likely to harbor pathologic pT0-1, pT2, pT3, or pT4 stage disease, which is determined after cystectomy.[4] Similarly, approximately 30% of patients with clinically negative pelvic lymph nodes are found to have pathologically positive pelvic lymph nodes after surgical dissection.

Although pelvic node involvement is strongly correlated with postoperatively determined T stage, there is almost no correlation with preoperative T stage.[4] There is also a stark discordance between the pre- and post-operative localization of tumors within subsites of the bladder. Approximately half of patients with cystectomy will harbor invasive tumors in subsites of the bladder that appeared free of disease preoperatively.[5] Overall, inadequate staging limits rational treatment planning and leads to the overtreatment of some patients and undertreatment of others.

In current practice, cystoscopy, tissue analysis from the transurethral resection of the bladder tumor, pelvic computed tomography (CT), and magnetic resonance imaging (MRI) are the primary modalities used to clinically stage patients with bladder cancer.[6] MRI is the most promising imaging method and has been shown to be sensitive to and specific for the detection and localization of macroscopic disease.[7-21] However, current MRI techniques are not able to detect microscopic tumor sites and qualitatively differentiate reactive changes after transurethral resection from sites of residual tumor.[22-30]

We undertook this study with the goal to develop an MRI-based radiomics algorithm that may be used to improve clinical staging and guide treatment. To our knowledge, quantitative image analysis to better predict the extent of invasion and location of bladder cancer from MRI scans has not been performed previously. We hypothesized that a quantitative image analysis with an optimal biomarker approach on the basis of features that are extracted from T2-weighted MRI scans can accurately classify ≤T2 versus >T2 invasion both at the patient level and within subsectors of the bladder.

Methods and materials

Patient characteristics

This retrospective study was approved by the institutional review board at our institution. Pelvic axial, T2-weighted, fast-spin, echo MRI data sets without gross motion artifacts acquired on 1.5 to 3.0 Tesla clinical MRI scanners from 65 consecutive adult patients with bladder cancer who underwent a cystectomy and histopathologic assessment (47 men, 18 women; mean age 65.6 ± 10.5 years) between 2009 and 2015 were utilized for this study. The image sizes varied from 268×208 to 512×448 with 23 to 65 slices and the voxel sizes varied from $0.62 \times 0.62 \times 4$ mm^3 to $1.48 \times 1.48 \times 12$ mm^3. The repeti-

tion time ranged from 1000 msec to 6680 msec and the echo time from 80 mse to 93 msec.

Among a total of 65 patients, 4 patients were imaged prior to transurethral resection of bladder tumor (TURBT), 27 patients were imaged after TURBT but prior to chemotherapy treatment, and 34 patients were imaged after TURBT and chemotherapy. A reference standard T-stage for each radial sector and each patient was determined by a board-certified radiologist (DAT) on the basis of a qualitative assessment of the T2-weighted MRI scans and use of available histopathology data from cystectomy specimens.

At the patient level, 31 patients were assigned to group 1 (stage ≤T2 with primary tumor that was locally confined to the bladder) and 34 patients to group 2 (stage >T2 with primary tumor that was locally extending beyond the bladder). In particular, 10 patients were stage T0, 3 patients stage Ta, 5 patients stage Tis, 5 patients stage T1, 8 patients stage T2, 24 patients stage T3 (16 patients T3a and 8 patients T3b), and 10 patients stage T4 (7 patients T4a and 3 patients T4b) on the basis of a histopathologic assessment after cystectomy.

At the sector level (where each patient study was divided into 8 equal sectors), 401 sectors were assigned to group 1 and 119 sectors to group 2. In particular, 289 sectors were stage T0, 3 sectors stage Ta, 18 sectors stage Tis, 29 sectors stage T1, 62 sectors stage T2, 88 sectors stage T3 (52 sectors T3a and 36 sectors T3b), and 31 sectors stage T4 (17 sectors T4a and 14 sectors T4b).

Three-dimensional region of interest placement and image intensity standardization

All image data sets were trimmed in a consistent manner for body region of interest (ROI) by using a computer-assisted visualization and analysis software system.[31] The axial slice with the maximal cross-sectional coverage through the femoral heads was selected. An ROI rectangular box in 3 dimensions was specified along the lateral edges of the femoral heads and anterior and posterior boundaries of the pelvic wall skeletal musculature.

Subseqwuently, all axial slices through the pelvis were trimmed by the same ROI. The two axial slices within 10 mm of the superior and inferior aspects of the urinary bladder were selected as the superior and inferior boundaries of the ROI, respectively. To ensure the same tissue-specific, numeric meaning for image voxel intensity values, all images were first corrected for intensity nonuniformities and then standardized[32-34] in accordance with a standard intensity scale. The parameters of the scale were estimated from 10 control (normal) MRI data sets.

Three-layer, shell-like volume of interest and radial sector placement

The visual appearance and image content of urine within the bladder lumen, bladder wall including the tumor sites, and perivesical fat on T2-weighted MRI scans are different as shown in Figure 1a. We postulated that the differential features that were extracted from these different regions can be utilized to determine bladder cancer T stage.

To classify patients into the 2 T-stage groups, a 3-layer shell-like volume of interest (VOI) was placed about the urinary bladder as shown in Figures 1b and 2. This includes an inner shell (containing high T2-weighted signal intensity urine within the bladder lumen), a middle shell (containing low-signal intensity bladder wall that is predominantly comprised of detrusor muscle and slightly higher-signal intensity foci of bladder tumor), and an outer shell (containing high-signal intensity perivesical fat that extends up to 10 mm out from the outer aspect of the bladder wall). The inner and outer boundaries of the bladder wall were manually drawn using a computer-assisted visualization and analysis software system on axial T2-weighted MRI scans by 2 trained individuals (JC, SV) so that the 3 shells could be created.

After creating the shells, we further divided each shell automatically into 8 equally spaced radial sectors (S1-S8) as shown in Figure 2. This figure also shows an example of the 3-layer, shell-like structure and radial sectors that were placed on a T2-weighted MRI scan about the urinary

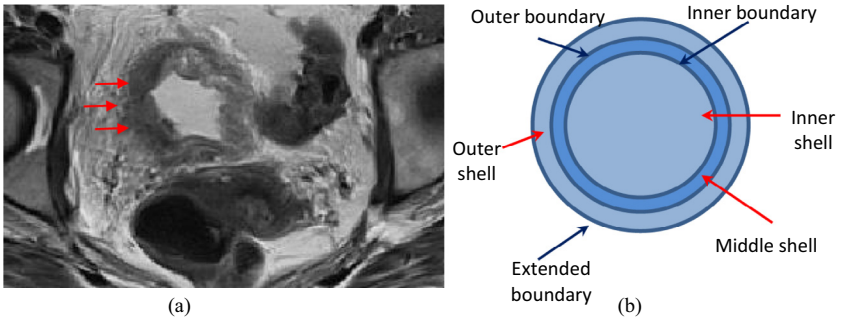

Figure 1 (a) The Visual appearance of bladder wall (arrows) on T2-weighted magnetic resonance imaging scan. (b) Schematic diagram of 3-layer, shell-like structure including boundaries and 8 radial sectors.

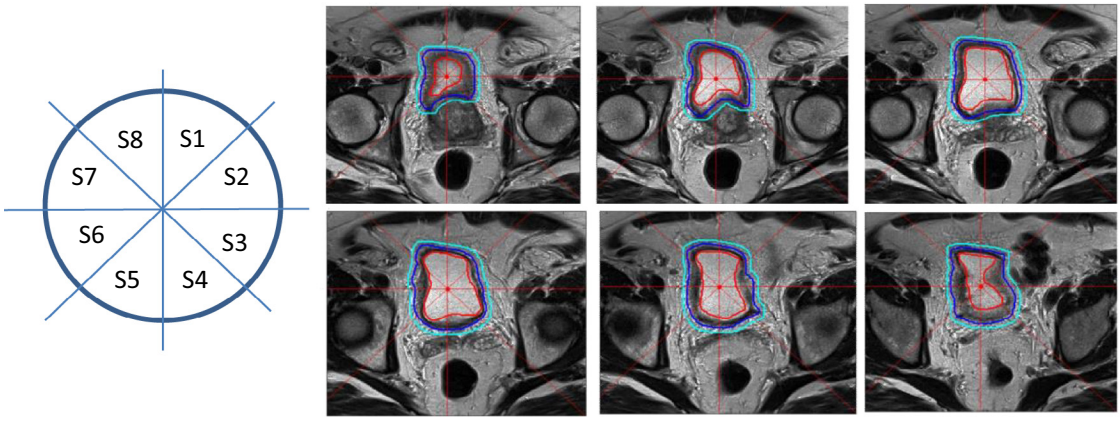

Figure 2 Three-layer, shell-like structure and 8 radial sectors placed about the bladder on serial T2-weighted magnetic resonance imaging scan in representative patient.

bladder in 1 patient that covered the full extent of the VOI (6 slices) as specified for this patient. This enabled a comparison of the proposed approach for bladder cancer T-staging at both the patient and radial-sector levels. The sector-level analysis was carried out in the 3-dimensional sector. For illustration in Figure 2, the first 3-dimensional sector that corresponds to S1 is comprised of the 2-dimensional, wedge-shaped regions that are labeled S1 from the 6 slices stacked together. Thus, each patient data set yielded 8 3-dimensional sectors. Of note, each 3-dimensional sector itself consisted of 3 shells.

Feature extraction, optimal biomarker selection, and cross-validation

A variety of image-based features including intensity and texture properties were extracted from each radial sector and each shell for all patients. The texture information included the local binary pattern (LBP) and those derived from gray level cooccurrence matrix (GLCM).[35] From GLCM, we used 6 texture properties including energy, maximum probability, contrast, inverse difference moment, and correlation.[36] Four different versions of LBP features were computed including the original LBP,[37] median LBP,[38] uniform LBP,[39] and neighbor-intensity LBP.[40]

After the intensity and texture feature sets were extracted for the 3 shells at the patient and sector levels, a recently developed optimal biomarker approach was used to extract a small optimal feature set.[41] The idea behind this approach was to find a small set of discriminating features from the set of all features in several steps as follows: 1) Extract a subset of features that have a low level of correlation among all features. A heat map visualization technique that allows for the grouping of parameters on the basis of correlations among them was used for this purpose; 2) independently of step 1, extract a subset of features from the entire set that is capable of separating the 2 patient groups of interest. Each feature is tested on its own for ability to separate groups by using *t* tests; and 3) find the intersection of these 2 subsets to generate the final small feature set.

The accuracy of the selected features to perform a classification of the new images into the 2 classification groups was tested with a leave-one-out strategy. A support vector machine was used as the classifying engine. Testing data sets in the leave-one-out strategy has no intersection with the training data sets that are used for optimal feature selection and support vector machine classification. Sensitivity, specificity, accuracy of prediction, and area under the receiver operating characteristic (ROC) curve were computed to describe the predictive performance of the optimal feature sets that consisted of different numbers of optimal features.

Results

Feature selection and classification

Each patient had 3 shells, each of which was further divided into 8 sectors for a total of 24 sectors per patient. Each sector yielded 42 intensity properties, 672 LBP texture properties, and 15,120 GLCM texture properties for a total of 15,834 features per sector. Figure 3 shows the correlations among all features using the heat map visualization technique. Vertical features in the red box include cooccurrence, matrix-based, texture features for the middle shell of sector 2. The horizontal features in the red box include cooccurrence, matrix-based, texture features for the inner shell of sector 2. Features from the middle shell of sector 2 do not much correlate with those from its inner shell.

The size of the selected optimal feature set can be varied by changing the amount of residual correlation allowed and

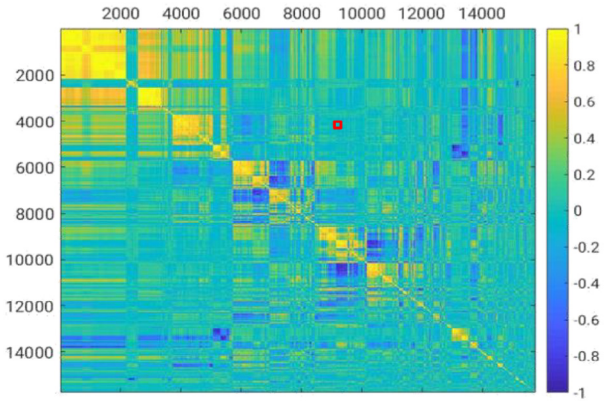

Figure 3 Heat map of feature correlation matrix.

the percent of top highly uncorrelated features we desire to select for this residual correlation.[41] The optimal biomarker feature sets from a minimum of 9 features to a maximum of 18 features were selected in this manner and analyzed. Table 1 shows the optimal biomarker feature set with 9, 14, and 18 features and the corresponding performance measures of sensitivity, specificity, prediction accuracy, and area under the ROC curve at both the patient and sector levels. Figure 4 shows ROC curves at the sector and patient levels for the 3 optimal feature sets. The best classification accuracy was produced by using 9 optimal features at both the sector and patient levels (Table 2).

Discussion

Classifying extent of invasion is crucial for treatment planning

The inability to accurately determine the extent of invasion of bladder cancer and its locations within the bladder with routine clinical staging methods affects appropriate treatment planning and may lead to the overtreatment of some patients and undertreatment of others. In this study, we focused on the binary classification of the presence or absence of extra-vesicle invasion because this distinction has been shown to be a strong predictor of occult pelvic lymph node involvement,[4] pelvic failure after surgery,[5] disease-free survival, and overall survival.[42] The accurate classification of extra-vesicle invasion could help clinicians make more prudent decisions with regard to the treatment of patients with neoadjuvant chemotherapy, chemoradiation, cystectomy, and pelvic lymph node dissection.

Table 1 Classification performance for bladder cancer T-staging on the basis of T2-weighted magnetic resonance imaging scan at sector and patient levels

	Sector level				Patient level			
No. of features	SEN	SPE	ACC	AUC	SEN	SPE	ACC	AUC
9	0.681	0.788	0.763	0.813	0.742	0.824	0.785	0.806
14	0.790	0.748	0.758	0.816	0.742	0.765	0.754	0.798
18	0.782	0.728	0.740	0.818	0.806	0.735	0.769	0.793

ACC, accuracy of prediction; AUC, area under receiver operating characteristic curve; SEN, sensivitity; SPE, specificity.

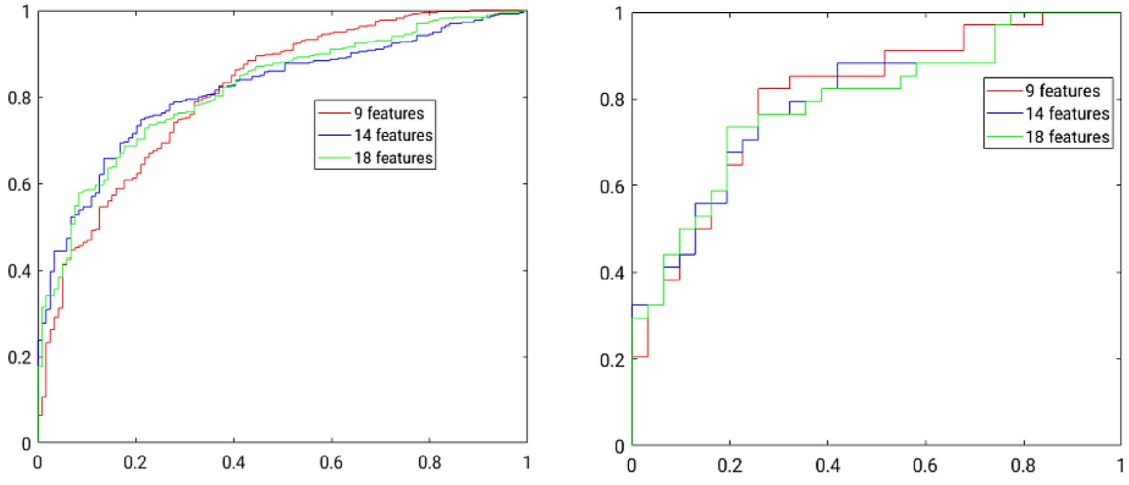

Figure 4 Receiver operating characteristic curves to classify bladder cancer at sector level (left) and patient level (right).

Table 2 Optimal biomarker set with 9 selected features extracted from middle shell and constituting texture properties

1	**Kurtosis from uniform LBP with radius 3 and neighborhood 8**
2	Kurtosis from uniform LBP with radius 3 and neighborhood 12
3	Median from contrast GLCM with window size 3x3 at 360° angle, bins 5, and radius 3
4	Median from contrast GLCM with window size 5x5 at 360° angle, bins 5, and radius 3
5	High quartile from correlation GLCM with window size 7x7 at 270° angle, bins 5, and radius 2
6	High quartile from contrast GLCM with window size 3x3 at 45° angle, bins 5, and radius 3
7	High quartile from contrast GLCM with window size 5x5 at 45° angle, bins 5, and radius 3
8	High quartile from correlation GLCM with window size 7x7 at 270° angle, bins 5, and radius 3
9	High quartile from contrast GLCM with window size 5x5 at 45° angle, bins 10, and radius 3

GLCM, grey level cooccurrence matrix; LBP, local binary pattern.

We used an optimal biomarker approach to identify features that were extracted from T2-weighted MRI scans that can classify extra-vesicle invasion both at the patient level and within subsectors of the bladder. With a 64-patient training set and using features from T2-weigthed MRI sequences alone, our algorithm demonstrated a sensitivity, specificity, accuracy of prediction, and area under ROC curve of 0.742, 0.824, 0.785, and 0.806, respectively, at the patient level and 0.681, 0.788, 0.763, and 0.813, respectively, at the radial sector level.

To our knowledge, this is the first study of its kind to assess the clinical staging of bladder cancer using MRI features and our findings set a benchmark for an MRI-based radiomics classification of the extent of invasion of bladder cancer. Prior work indicates that the performance of traditional imaging methods in staging bladder cancer is subpar. CT and MRI have been shown to be inaccurate in up to 50% of cases.[21-23] TURBT also understages tumors in up to 50% of patients.[24-30]

A limitation of our classification algorithm is that it does not make more granular distinctions with respect to the extent of invasion other than extra-vesicle invasion versus no extra-vesicle invasion. More granular distinctions are important as, for example, patients with superficial invasion alone (ie, T1) can be effectively treated with less rigorous therapy than those with invasion into the muscle and beyond. Another example is the subset of patients who may be cured with diagnostic TURBT alone (T0). Although the present analysis did not attempt to delineate more granular stages, the analytic approach that was used in this study could naturally extend to these other clinically important classification stages in future studies.

Optimal biomarker approach allows for clinically driven radiomics

In this study, we created a 3-layer, shell-like VOI around the bladder and generated a feature set for each shell on T2-weighted MRI scans. We designed and computed a large collection of features and extracted a small subset of this collection using an optimal biomarker approach, which maximizes feature independence and classification potential.[41]

Deep learning is an alternative approach and has been utilized in bladder cancer segmentation and treatment-response assessment from CT images.[43-45] Deep learning is similar to the optimal biomarker approach because a large number of features are examined by the network depending on the needs and characteristics of the training data sets for the classification or prediction problem[43] but these features are designed by the network and not the user. The advantage of the optimal biomarker method is that this method can reduce the dimensionality of the feature set while keeping the original meaning of the features so all selected features can be explained and repeatedly computed.

In contrast, it is hard to finally determine quantitatively what physical features (as those listed in Table 2) are actually utilized by the network in deep learning to make its decision. This may hinder the process of potentially studying cancer pathophysiology utilizing the physical meaning of the selected features.

Magnetic resonance imaging is a promising modality for further development

Recent research on bladder cancer staging from CT images reported that the use of morphological and texture features and machine-learning techniques to stratify bladder cancer into stage categories shos the promise of feature selection and classification to predict bladder cancer status from medical imaging.[46,47] Positron emission tomography and CT images have also been studied recently with respect to the classification of bladder primaries but with mixed results compared with CT and MRI-based approaches.[48,49]

However, in our view, MRI has important advantages over CT-based modalities. First, MRI does not expose patients to ionizing radiation; thus, numerous sequences can be performed without concern for late effects from radiation exposure. Second, each sequence can potentially provide additional anatomic and biologic information that can further improve the accuracy of classification algorithms. In this study, we considered only T2-weighted sequences. Our results would likely improve when information from the T2-weighted scans were combined with T1-weighted, diffusion, and other biologically meaningful sequences. Future research can extend this initial work in this direction.

Our study has certain limitations. Most notably, the classification algorithms developed herein were trained on a

small number of samples and have not been externally validated. Although the performance of these algorithms is very promising, there is a chance that they have overfitted the training data. As a next step in this research, we plan to assess performance in additional patients from our own institution as well as from other institutions.

Conclusions

This is the first study to demonstrate a highly accurate classification of extra-vesicle invasion using an optimal biomarker approach on features that were extracted from T2-weighted MRI scans. The derived features performed well at both the patient level and within subsectors of the bladder. The methods used herein have the potential to be extended and incorporate information from additional MRI sequences and address other clinically important classification problems in bladder cancer.

References

1. Siegel RL, Miller KD, Jemal A. Cancer statistics, 2017. *CA Cancer J Clin*. 2017;67:7-30.
2. Gschwend JE, Heck MM, Lehmann J, Ruebben H, Albers P, Heidenreich A. Limited versus extended pelvic lymphadenectomy in patients with bladder cancer undergoing radical cystectomy: Survival results from a prospective, randomized trial (LEA AUO AB 25/02). *J Clin Oncol*. 2016;34:4503.
3. Michaelson MD, Hu C, Pham HT, et al. A phase 1/2 trial of a combination of paclitaxel and trastuzumab with daily irradiation or paclitaxel alone with daily irradiation after transurethral surgery for noncystectomy candidates with muscle-invasive bladder cancer (Trial NRG Oncology RTOG 0524). *Int J Radiat Oncol Biol Phys*. 2017;97:995-1001.
4. Goldsmith B, Baumann BC, He J, et al. Occult pelvic lymph node involvement in bladder cancer: Implications for definitive radiation. *Int J Radiat Oncol Biol Phys*. 2014;88:603-610.
5. Goldsmith B, Tucker K, Conway RG, et al. Discordance between preoperative and postoperative bladder cancer location: Implications for partial-bladder radiation. *Int J Radiat Oncol Biol Phys*. 2013;85:707-713.
6. Vargas HA, Akin O, Schoder H, et al. Prospective evaluation of MRI, (1)(1)C-acetate PET/CT and contrast-enhanced CT for staging of bladder cancer. *Eur J Radiol*. 2012;81:4131-4137.
7. Ghafoori M, Shakiba M, Ghiasi A, Asvadi N, Hosseini K, Alavi M. Value of MRI in local staging of bladder cancer. *Urol J*. 2013;10:866-872.
8. Wu LM, Chen XX, Xu JR, et al. Clinical value of T2-weighted imaging combined with diffusion-weighted imaging in preoperative T staging of urinary bladder cancer: A large-scale, multi-observer prospective study on 3.0-T MRI. *Acad Radiol*. 2013;20:939-946.
9. Nishimura K, Fujiyama C, Nakashima K, Satoh Y, Tokuda Y, Uozumi J. The effects of neoadjuvant chemotherapy and chemo-radiation therapy on MRI staging in invasive bladder cancer: Comparative study based on the pathological examination of whole layer bladder wall. *Int Urol Nephrol*. 2009;41:869-875.
10. Robinson P, Collins CD, Ryder WD, et al. Relationship of MRI and clinical staging to outcome in invasive bladder cancer treated by radiotherapy. *Clin Radiol*. 2000;55:301-306.
11. Rajesh A, Sokhi HK, Fung R, Mulcahy KA, Bankart MJ. Bladder cancer: Evaluation of staging accuracy using dynamic MRI. *Clin Radiol*. 2011;66:1140-1145.
12. Watanabe H, Kanematsu M, Kondo H, et al. Preoperative T staging of urinary bladder cancer: Does diffusion-weighted MRI have supplementary value? *AJR Am J Roentgenol*. 2009;192:1361-1366.
13. Tekes A, Kamel I, Imam K, et al. Dynamic MRI of bladder cancer: Evaluation of staging accuracy. *AJR Am J Roentgenol*. 2005;184:121-127.
14. Rabie E, Faeghi F, Izadpanahi MH, Dayani MA. Role of dynamic contrast-enhanced magnetic resonance imaging in staging of bladder cancer. *J Clin Diagn Res*. 2016;10:TC1-TC5.
15. Zhou G, Chen X, Zhang J, Zhu J, Zong G, Wang Z. Contrast-enhanced dynamic and diffusion-weighted MR imaging at 3.0T to assess aggressiveness of bladder cancer. *Eur J Radiol*. 2014;83:2013-2018.
16. Nguyen HT, Jia G, Shah ZK, et al. Prediction of chemotherapeutic response in bladder cancer using K-means clustering of dynamic contrast-enhanced (DCE)-MRI pharmacokinetic parameters. *J Magn Reson Imaging*. 2015;41:1374-1382.
17. Nguyen HT, Pohar KS, Jia G, et al. Improving bladder cancer imaging using 3-T functional dynamic contrast-enhanced magnetic resonance imaging. *Invest Radiol*. 2014;49:390-395.
18. Naish JH, McGrath DM, Bains LJ, et al. Comparison of dynamic contrast-enhanced MRI and dynamic contrast-enhanced CT biomarkers in bladder cancer. *Magn Reson Med*. 2011;66:219-226.
19. Bains LJ, McGrath DM, Naish JH, et al. Tracer kinetic analysis of dynamic contrast-enhanced MRI and CT bladder cancer data: A preliminary comparison to assess the magnitude of water exchange effects. *Magn Reson Med*. 2010;64:595-603.
20. Tuncbilek N, Kaplan M, Altaner S, et al. Value of dynamic contrast-enhanced MRI and correlation with tumor angiogenesis in bladder cancer. *AJR Am J Roentgenol*. 2009;192:949-955.
21. Srivastava A, Douglass LM, Chernyak V, Watts KL. Advances in imaging in prostate and bladder cancer. *Curr Urol Rep*. 2017;18:69.
22. Zlatev DV, Altobelli E, Liao JC. Advances in imaging technologies in the evaluation of high-grade bladder cancer. *Urol Clin North Am*. 2015;42:147-157, vii.
23. Hafeez S, Huddart R. Advances in bladder cancer imaging. *BMC Med*. 2013;11:104.
24. Jewett HJ, Strong GH. Infiltrating carcinoma of the bladder; relation of depth of penetration of the bladder wall to incidence of local extension and metastases. *J Urol*. 1946;55:366-372.
25. MacVicar AD. Bladder cancer staging. *BJU Int*. 2000;86:111-122.
26. Stein JP, Lieskovsky G, Cote R. Radical cystectomy in the treatment of invasive bladder cancer: Long-term results in 1,054 patients. *J Clin Oncol*. 2001;19:666-675.
27. Dutta SC, Smith JA Jr, Shappell SB, Coffey CS, Chang SS, Cookson MS. Clinical under staging of high risk nonmuscle invasive urothelial carcinoma treated with radical cystectomy. *J Urol*. 2001;166:490-493.
28. Ficarra V, Dalpiaz O, Alrabi N, Novara G, Galfano A, Artibani W. Correlation between clinical and pathological staging in a series of radical cystectomies for bladder carcinoma. *BJU Int*. 2005;95:786-790.
29. Mehrsai A, Mansoori D, Taheri Mahmoudi M, Sina A, Seraji A, Pourmand GH. A comparison between clinical and pathologic staging in patients with bladder cancer. *Urol J*. 2004;1:85-89.
30. Miladi M, Peyromaure M, Zerbib M, Saighi D, Debre B. The value of a second transurethral resection in evaluating patients with bladder tumours. *Eur Urol*. 2003;43:241-245.
31. Grevera G, Udupa J, Odhner D, et al. CAVASS: A computer-assisted visualization and analysis software system. *J Digit Imaging*. 2007;20:101-118.
32. Nyul LG, Udupa JK. On standardizing the MR image intensity scale. *Magn Reson Med*. 1999;42:1072-1081.
33. Zhuge Y, Udupa JK, Liu J, Saha PK. Image background inhomogeneity correction in MRI via intensity standardization. *Comput Med Imaging Graph*. 2009;33:7-16.

34. Madabhushi A, Udupa JK. Interplay between intensity standardization and inhomogeneity correction in MR image processing. *IEEE Trans Med Imaging*. 2005;24:561-576.
35. Haralick RM, Shanmugam K. Textural features for image classification. *IEEE Trans Syst Man Cybernet*. 1973;6:610-621.
36. Sonka M, Hlavac V, Royle R. Image processing, analysis, and machine vision. Cen-gage Learning, 2014.
37. Ojala T, Pietikainen M, Harwood D. Performance evaluation of texture measures with classification based on Kullback discrimination of distributions. In: *Pattern Recognition, Conference A: Computer Vision & Image Processing*, Vol. 1. IEEE; 1994:582-585.
38. Liu L, Lao S, Fieguth PW, Guo Y, Wang X, Pietikainen M. Median robust extended local binary pattern for texture classification. *IEEE Trans Image Process*. 2016;25:1368-1381.
39. Ojala T, Pietikainen M, Maenpaa T. Multiresolution gray-scale and rotation invariant texture classification with local binary patterns. *IEEE Trans Pattern Anal Machine Intel*. 2002;24:971-987.
40. Li L, Fieguth PW, Kuang G. Generalized local binary patterns for texture classification. *BMVC*. 2011;1-11.
41. Tong Y, Udupa JK, Sin S, et al. MR Image analytics to characterize the upper airway structure in obese children with obstructive sleep apnea syndrome. *PLoS ONE*. 2016;11:e0159327.
42. Campi R, Minervini A, Mari A, et al. Anatomical templates of lymph node dissection for upper tract urothelial carcinoma: A systematic review of the literature. *Expert Rev Anticancer Ther*. 2017;17:235-246.
43. Cha KH, Hadjiiski L, Chan HP, et al. Bladder cancer treatment response assessment in CT using radiomics with deep-learning. *Sci Rep*. 2017;7:8738.
44. Cha KH, Hadjiiski LM, Samala RK, et al. Bladder cancer segmentation in CT for treatment response assessment: Application of deep-learning convolution neural network-a pilot study. *Tomography*. 2016;2:421-429.
45. Cha KH, Hadjiiski L, Samala RK, Chan HP, Caoili EM, Cohan RH. Urinary bladder segmentation in CT urography using deep-learning convolutional neural network and level sets. *Med Phys*. 2016;43:1882.
46. Garapati SS, Hadjiiski L, Cha KH, et al. Urinary bladder cancer staging in CT urography using machine learning. *Med Phys*. 2017;44:5814-5823.
47. Wang G, Lam KM, Deng Z, Choi KS. Prediction of mortality after radical cystectomy for bladder cancer by machine learning techniques. *Comput Biol Med*. 2015;63:124-132.
48. Brunocilla E, Ceci F, Schiavina R, et al. Diagnostic accuracy of (11)C-choline PET/CT in preoperative lymph node staging of bladder cancer: A systematic comparison with contrast-enhanced CT and histologic findings. *Clin Nucl Med*. 2014;39:e308-e312.
49. Nayak B, Dogra PN, Naswa N, Kumar R. Diuretic 18F-FDG PET/CT imaging for detection and locoregional staging of urinary bladder cancer: Prospective evaluation of a novel technique. *Eur J Nucl Med Mol Imaging*. 2013;40:386-393.